Bioorganic Chemistry 82 (2019) 405–413

Contents lists available at ScienceDirect

Bioorganic Chemistry

journal homepage: www.elsevier.com/locate/bioorg

Side-chain cleaved phytoecdysteroid metabolites as activators of protein kinase B

Halima Meriem Issaadi[a], József Csábi[a], Tusty-Jiuan Hsieh[b], Tamás Gáti[c], Gábor Tóth[a,d,*], Attila Hunyadi[a,e,*]

[a] Institute of Pharmacognosy, Interdisciplinary Excellence Center, University of Szeged, Eötvös str. 6, 6720 Szeged, Hungary
[b] Graduate Institute of Medicine, Kaohsiung Medical University, Kaohsiung 807, Taiwan, Republic of China
[c] Servier Research Institute of Medicinal Chemistry (SRIMC), Záhony utca 7, H-1031 Budapest, Hungary
[d] NMR Group, Department of Inorganic and Analytical Chemistry, University of Technology and Economics, Szt. Gellért Sq. 4, H-1111 Budapest, Hungary
[e] Interdisciplinary Centre for Natural Products, University of Szeged, Eötvös str. 6, 6720 Szeged, Hungary

ARTICLE INFO

Keywords:
Ecdysteroids
In vivo metabolism
Hypervalent iodine chemistry
Base-catalyzed autoxidation
Akt phosphorylation
NMR
Stereo structure

ABSTRACT

Phytoecdysteroids exert their non-hormonal anabolic and adaptogenic effects in mammals, including humans, through a partially revealed mechanism of action involving the activation of protein kinase B (Akt). We have recently found that poststerone, a side-chain cleaved *in vivo* metabolite of 20-hydroxyecdysone, exerts potent anabolic activity in rats.

Here we report the semi-synthetic preparation of a series of side-chain cleaved ecdysteroids and their activity on the Akt phosphorylation in murine skeletal muscle cells. Twelve C-21 ecdysteroids including 8 new compounds were obtained through the oxidative side-chain cleavage of various phytoecdysteroids, or through the base-catalyzed autoxidation of poststerone. The complete ^{1}H and ^{13}C NMR spectroscopic assignments of the new compounds are presented. Among the tested compounds, 9 could activate Akt stronger than poststerone revealing that side-chain cleaved derivatives of phytoecdysteroids other than 20-hydroxyecdysone are valuable bioactive metabolites. Thus, our results suggest that the expectable *in vivo* formation of such compounds should contribute to the bioactivity of herbal preparations containing ecdysteroid mixtures.

1. Introduction

The global phenomenon of population ageing directs an increasing attention towards natural approaches to maintain health and strength in general, and supplementation with herbal adaptogens and/or natural anabolic agents provides an attractive way to achieve this. Phytoecdysteroids are among the most popular options in this regard.

Ecdysteroids are a large and diverse family of polyhydroxylated sterols; there are more than 500 representatives of these compounds currently known to occur in Nature [1]. Concerning their chemistry, most of them possess a C_{27} carbon skeleton derived biosynthetically from cholesterol. However, the number of carbon atoms can vary. Ecdysteroids occur as C_{27}, C_{28}, or C_{29} compounds if the whole sterol-type side chain is present, or they can be C_{19}, C_{21}, or C_{24} compounds if a partial or complete metabolic side-chain cleavage takes place between C_{17}-C_{20}, C_{20}-C_{22} or C_{24}-C_{25}, respectively. Most of the naturally occurring phytoecdysteroids possess a 7-en-6-one chromophore group in the ring B. The A/B ring junction is normally *cis*, whereas the B/C and C/D ring junctions are almost always *trans* [2].

Ecdysteroids were initially discovered as the molting hormones of insects [3], but soon after they were also isolated from Plant Kingdom, where their concentration can reach as much as 1,000-fold higher than that typically found in arthropods [4]. Phytoecdysteroids can reach as much as 2–3% of the dry weight in some species (e.g. seeds of *Rhaponticum carthamoides* and stalks of *Diploclisia glaucescens*, inflorescences of *Serrulata inermis* and roots of *Cyanotis arachnoidea*) [5]. It is important to note that while plants' ecdysteroid composition is typically dominated by a few major ecdysteroids (usually 20-hydroxyecdysone; 20E), a complex cocktail of minor compounds is generally present whose bioactivity needs to be taken into account when ecdysteroid-containing herbal preparations are used.

It is generally accepted that phytoecdysteroids do not interact with the vertebrate steroid hormone system. Still, they exert numerous beneficial effects on mammals (e.g. anabolic, adaptogenic, antidiabetic, hypolipidemic, hepatoprotective, etc.), while their acute toxicity is negligible [4–10]. Phytoecdysteroids have long been known for their

* Corresponding authors at: Institute of Pharmacognosy, Interdisciplinary Excellence Center, University of Szeged, Eötvös str. 6, 6720 Szeged, Hungary.
E-mail addresses: drtothgabor@t-online.hu (G. Tóth), hunyadi.a@pharm.u-szeged.hu (A. Hunyadi).

https://doi.org/10.1016/j.bioorg.2018.10.049
Received 26 July 2018; Received in revised form 10 September 2018; Accepted 24 October 2018
Available online 31 October 2018
0045-2068/

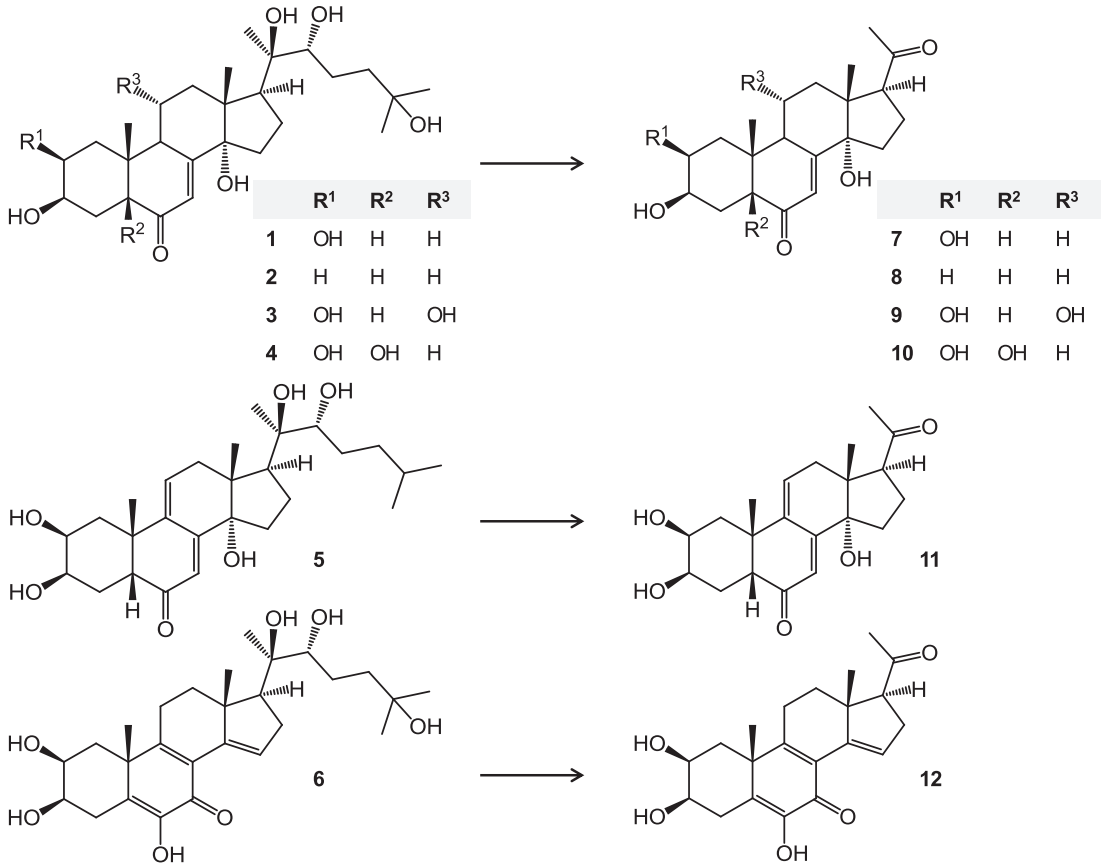

Fig. 1. Preparation of ecdysteroid derivatives through oxidative side-chain cleavage.

complex bioactivity that could be referred to as a broad-spectrum, general strengthening effect. Several *in vitro* and *in vivo* studies confirmed the anabolic activity of ecdysteroids that is characterized by an increase in growth and skeletal muscle mass [11–12], as well as in the fiber size through muscle-specific effects [13] in different animals. The exact mechanism of action behind this anabolic activity is only partially understood, and needs further clarification. Recently, Gorelick-Feldman et al. found that 20E (**1**) caused a hasty elevation in intracellular calcium levels, leading to a maintained activation of protein kinase B (Akt) and to an increased protein synthesis in a mouse skeletal muscle cell line (C2C12) [14]. Protein kinase B and its downstream effectors, inter alia, represent a major signaling pathway that controls protein turnover in skeletal muscles, and this function appears to be maintained in ageing muscles as well [15–16]. This role makes it an appropriate target to test ecdysteroids for their anabolic "strengthening" potential. Activity on this pathway can also provide indirect information on the capacity of ecdysteroids to promote muscle gain and/or prevent muscle loss.

The possible role of *in vivo* metabolites of ecdysteroids in the observed bioactivities has long been part of related scientific discussion. Recent studies of Kumpun et al. identified several metabolites in the urine and feces of mice treated by an intraperitoneal injection of 20E (**1**) [17]. Side chain cleavage between C-20 and C-22, and dehydroxylation at C-14 were identified as major metabolic steps, thus yielding poststerone (**7**), 14-deoxy-20-hydroxyecdysone and 14-deoxypoststerone, which then undergo a reductive metabolism in several further steps [17]. We have recently found that poststerone (**7**) acts as a potent anabolic agent on rat skeletal muscles *in vivo*, implying that it plays an important role in the *in vivo* anabolic activity of its parental compound 20E (**1**) (unpublished results; manuscript by Csábi et al. is currently under evaluation at Sci. Rep., first submission: 26.04.2018). Accordingly, it seems reasonable to assume that side-chain cleaved metabolites of phytoecdysteroids other than 20E (**1**) might also arise *in vivo*, and that these metabolites are also valuable bioactive compounds.

The base-catalyzed autoxidation of 20E (**1**), first described by Suksamrarn et al. in 1994 [18], was recently found by our research group to yield several oxidized derivatives exerting stronger activity on the Akt phosphorylation in murine skeletal muscle cells as compared to their parental compound 20E (**1**) [19]. This, together with the *in vivo* relevance of poststerone (**7**), led us to rise the following objectives for the present study: *(i)* to prepare a series of new C-21 ecdysteroid derivatives by using oxidative side-chain cleavage on various phytoecdysteroids or through the autoxidation of poststerone (**7**), and *(ii)* to evaluate the compounds' activity on the protein kinase B activation in murine skeletal muscle cells.

2. Results and discussion

2.1. Chemistry

2.1.1. Preparation of ecdysteroids 7–12 through oxidative side-chain cleavage

Oxidative side-chain cleavage of different phytoecdysteroids (**1–6**) was performed by using either the hypervalent iodine reagent [bis (trifluoroacetoxy)iodo]benzene (PIFA) or (diacetoxyiodo)benzene (PIDA).

Poststerone (**7**) was previously published to form when oxidizing 20E (**1**) with $NaIO_4$ (yield not reported) [20] or with Jones reagent (62% yield) [21]. Our recently published procedure, using PIFA for the same oxidation, could provide compound **7** in a yield of 57.8% [22]. In the present study, we report an update to this reaction: when using PIDA in a large-scale reaction followed by purification with flash

chromatography, poststerone (**7**) could be obtained in a decent isolated yield of 81.41%.

In order to obtain side-chain cleaved analogs (i.e. likely major *in vivo* metabolites) of other phytoecdysteroids, the reaction was also carried out on natural ecdysteroids with different substituents on the steroid skeleton, namely 2-deoxy-20-hydroxyecdysone (**2**), ajugasterone C (**3**), polypodine B (**4**), and dacryhainansterone (**5**) with the use of PIFA, and calonysterone (**6**) with the use of PIDA as reagent. Since these compounds were available in lower amounts than 20E (**1**), smaller scale reactions were performed. Preparative reverse-phase HPLC (RP-HPLC) was applied to obtain compounds **8** and **9**, rotation planar chromatography (RPC) was used to obtain compounds **10** and **11**, and centrifugal partition chromatography (CPC) was utilized to obtain compound **12**. Structures of the starting materials and their respective analogs are presented in Fig. 1.

For comparison purposes, reactions first performed with the use of PIFA as reagent were also carried out also by using PIDA instead. Less complex mixtures were obtained this way, and the expected products were obtained with the following yields: **8** (68.34%), **9** (63.57%), **10** (71.23%) and **11** (82.71%). Based on these comparative experiments, we could conclude that the use of PIDA as reagent instead of PIFA provides higher yields of the desired C-21 ecdysteroids. We hypothesize that the reason for this is decomposition due to by-product TFA that strongly acidifies the reaction medium when using PIFA, while acetic acid released by PIDA provides milder conditions leading to less complex mixtures and higher final yields of the target compounds.

2.1.2. Preparation of autoxidized derivatives 13–18 of poststerone (7)

Considering our previous observations on the significant bioactivity changes connected to certain autoxidized derivatives 20E (**1**) [19], our second aim was to prepare similar derivatives from poststerone (**7**), which would likely represent *in vivo* relevant metabolites of the corresponding analogs obtained from 20E (**1**). The base-catalyzed autoxidation of poststerone (**7**) was carried by dissolving the starting material in methanol - water (9:1, v/v) and subsequently NaOH was added to the mixture as a catalyst. The reaction mixture was stirred for 4 h, stopped by neutralizing the pH with 9.6% acetic acid, extracted through silica and dried. The dry residue was fractionated by centrifugal partition chromatography (CPC) in ascending mode, with a biphasic solvent system composed of ethyl acetate - water - methanol (20:20:1, v/v/v). Combined fractions were further purified by RP-HPLC to obtain compounds **13–18**. Compound **12** was also identified from this reaction, but its preparation from calonysterone (**6**) was more preferable due to the much higher yield. Structures of the synthesized derivatives (**13–18**) are presented in Fig. 2.

In order to allow biological testing of the isolated products, larger amounts were required. To achieve this, a set of small-scale reactions were performed, and the degradation of poststerone (**7**) and the formation of its oxidized derivatives (**12–18**) were monitored by normal phase (NP-TLC). As a result, we found that a longer reaction time of *ca.* 7–9 h is preferable to increase the yield of the targeted compounds. Thus, the same reaction was conducted for 7 h using 500 mg of poststerone (**7**), followed by the same purification steps as before. Yields of compounds **13**, **15**, **16** and **18** increased by 2.46, 1.59, 4.81, 1.10 times respectively. On the other hand, compound **17** was not detected anymore after 4 h.

2.2. Structure elucidation

Structure elucidation of the products was performed by means of comprehensive one- and two-dimensional NMR methods using widely accepted strategies [23–24], and we established the compounds' complete ^{1}H and ^{13}C signal assignment. Most ^{1}H assignments were accomplished using general knowledge of chemical shift dispersion with the aid of the ^{1}H–^{1}H coupling pattern (^{1}H NMR spectra). ^{1}H NMR chemical shifts of overlapped signals were identified by 2D HSQC and HMBC experiments, and by utilising 1D selective ROESY (Rotating frame Overhauser Enchancement Spectroscopy) responses or 1D selective TOCSY experiments.

Compounds **7**, **9** and **11** (poststerone, 11α-hydroxypoststerone and 9,11-didehydropoststerone, respectively) [22,25–26], were previously isolated and fully characterized by our research group; their ^{1}H and ^{13}C NMR chemical shifts correlated well with the values reported earlier. HPLC chromatograms and UV spectra of compounds **7**, **9** and **11** are available as Supplementary Information (Figs. S46, S48, and S50, respectively).

The ^{1}H and ^{13}C NMR chemical shifts of the eight new compounds (**8**, **10**, **12**, **14–18**), together with the data of poststerone as reference (**7**), are compiled in Table 1 and 2.

The side-chain cleavage of phytoecdysteroids (**1–6**) took place between the two hydroxylated carbon atoms C-20 and C-22, and led to the formation of a CH_3-C═O group attached to C-17 as it is straightforward

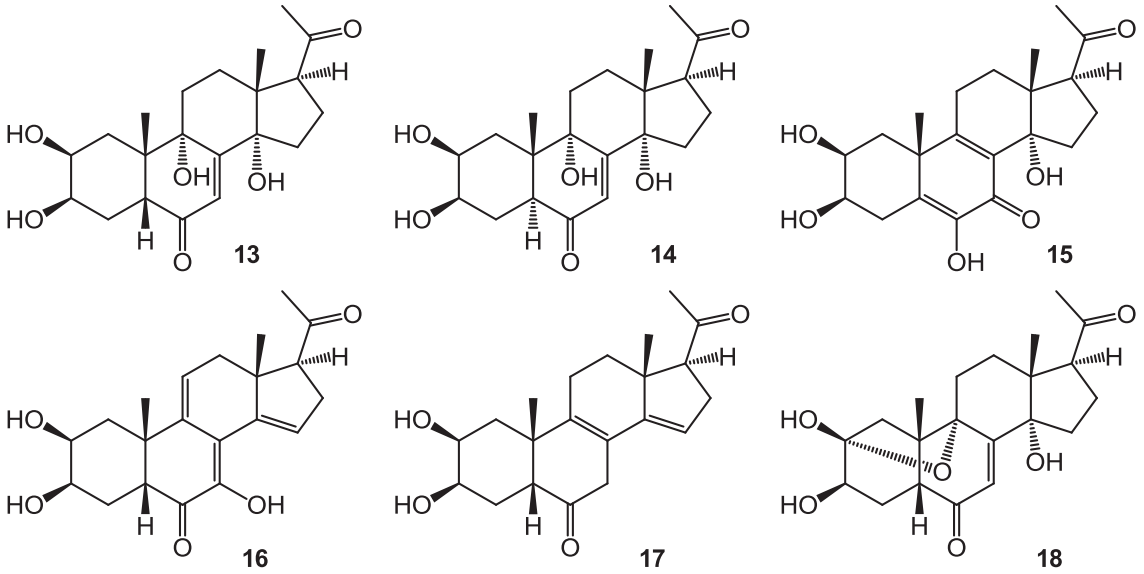

Fig. 2. Structure of the isolated compounds **13–18**.

Table 1
^{1}H chemical shift of compounds **7**, **8**, **10**, **12**, **14–18** in methanol-d_4 and **18** also in dimethyl sulfoxide-d_6 (**18**[a]).

Atom no.		7	8	10	12	14	15	16	17	18	18[a]
1	α	1.80	1.62	1.74*	1.38	2.17	1.46	2.03	1.93	1.96	1.84
	β	1.44	1.47	1.74*	2.44	1.71	2.32	1.70	1.62	2.21	2.08
2	α	3.86	1.81	3.96	4.01	4.01	4.01	3.77	3.48	–	–
	β	–	1.66	–	–	–	–	–	–	–	–
3		3.97	3.98	4.00	3.53	3.55	3.51	3.88	3.94	3.79	3.61
4	α	1.74	1.81	2.08	3.13	1.91	3.11	1.38	1.79	2.16	1.98
	β	1.74	1.57	1.78	2.54	1.75	2.53	1.80	1.70	1.81	1.61
5		2.39	2.44	–	–	3.17	–	2.62	2.49	2.43	2.29
7	α	5.82	5.81	5.87	–	5.84	–	–	3.33	5.76	5.64
	β	–	–	–	–	–	–	–	2.69	–	–
9		3.19	3.25	3.23	–	–	–	–	–	–	–
11	α	1.89	1.81	1.89	2.73	1.80	2.63*	6.04	2.41	2.06	1.97
	β	1.67	1.63	1.73	2.65	2.07	2.63*	–	2.41	1.81	1.62
12	α	2.33	2.32	2.33	1.74	2.36	2.26	2.52	1.80	2.35	2.21
	β	1.82	1.79	1.83	2.33	1.78	1.93	2.73	2.30	1.82	1.71
15	α	1.70	1.69	1.69	6.81	1.75	2.63	6.79	5.45	1.62	1.50
	β	2.00	2.02	2.00	–	1.97	2.00	–	–	1.94	1.84
16	α	1.88	1.90	1.88	2.38	1.87	1.90	2.46	2.31	1.89	1.72
	β	2.23	2.24	2.25	2.98	2.25	2.25	3.01	2.90	2.24	2.09
17		3.33	3.34	3.33	3.00	3.35	3.16	3.11	3.04	3.33	3.20
18		0.62	0.63	0.63	0.80	0.65	0.66	0.82	0.78	0.64	0.50
19		0.96	0.96	0.91	1.50	1.10	1.50	1.13	1.01	1.05	0.93
21		2.16	2.14	2.15	2.22	2.16	2.17	2.23	2.21	2.16	2.10

* Signals that are accidentally isochrones.
[a] OH signals of compound **18**: 2-OH 6.63 s; 3-OH 5.00 d 3.9 Hz; 14-OH 4.49 s.

from the δH$_3$-21 signals around 2.16 ppm, and the δC-21 and δC-20 peaks at ~31 and ~212 ppm, respectively (see Table 1 and 2). It should be mentioned that the ^{13}C signals of the steroid skeleton of the starting compounds showed only moderate changes upon side chain cleavage.

Compound **8** presented similar UV spectrum as its parental compound, 2-Deoxy-20-hydroxyecdysone (**2**), indicating no change in the chromophore. By means of MS, molecular weight of compound **8** was determined as $m/z = 347$ $[M + H]^+$, suggesting that the side-chain was successfully cleaved between C20-22, resulting in the molecular formula $C_{21}H_{30}O_4$. HPLC chromatogram and UV spectrum of compound **8** are available as Supplementary Information: Fig. S47, together with the NMR spectra: Fig. S1–Fig. S6. In the ^{1}H spectrum taken at 27 °C, some signals of the A/B rings appeared rather broadened, but when raising the temperature up to 50 °C they became sharp, and the bandwidth at half maximum of the H-3 signal changed from 21 Hz to 11 Hz, whereas the broad coalescence-like H-9 signal turned into a ddd multiplet with ^4J(H-9,H-7) = 2.5 Hz, ^3J(H-9,Hα-11) = 6.8 Hz and ^3J(H-9,Hβ-11) = 11.9 Hz couplings. Similar line-broadening was observed with the ^{13}C signals. Even at 50 °C, in the edited DEPTQ spectrum (Fig. S3), from the five CH atoms (upside signals), only four: C-7, C-3, C-17 and C-5 appeared, whereas C-9, around 35 ppm, remained under the noise level due to the strong broadening. The exact δC-9 = 35.5 ppm value was established from the H-9/C-9 cross-peak of HSQC spectrum (Fig. S4). Utilizing the edited HSQC spectrum (Fig. S5), the assignment of the two broad methylene signals (δC-11 = 22.1, δC-1 = 30.0 ppm) can also be verified. The HMBC spectrum (Fig. S6) provided H/C correlations ($^{2,3}J$(H,C) over two and three bonds, supporting the structure and the assignment even for the quaternary carbon atoms. Considering the inserted H$_3$-19/C and H$_3$-18/C section of HMBC, the cross-peaks of H$_3$-19 methyl hydrogens unambiguously assigned the quaternary C-10, tertiary C-5 and C-9, and secondary C-1 signals, and the H$_3$-18 hydrogens identified the quaternary C-13 and C-14, tertiary C-17 and secondary C-12 signals. Differentiation between the α/β positions of hydrogen atoms in the poststerone core, and also confirming the *cis*-type junction of the A/B rings were achieved through the one-dimensional selective ROESY experiments with irradiation of the H$_3$-18 and H$_3$-19 hydrogen atoms (Fig. S3). We have previously proven that, in case of studying ecdysteroids at 500 MHz frequency, this approach provide a sensitivity that strongly exceeds that of the analogous selective NOE (Nuclear Overhauser-Enhancement) experiment [27].

While in case of compound **8** we observed a temperature dependent signal broadening/sharpening, indicating a slow interconversion of different conformers, such a phenomenon did not occur in the case of poststerone (**7**). Such a different behavior of these compounds is likely due to the fact that in compound **7** the A ring of the 5β *cis*-linked A/B steroid frame predominantly appears in a chair conformation with equatorial HO-2 and axial HO-3 groups. Despite of the axial position of HO-3 group, the equatorial HO-2 substituent stabilizes this conformer. In compound **8**, however, there is only one unfavorable axial HO-group, allowing the appearance of such twisted-boat conformer(s) where the substituent is no more axial (see Fig. S5). The slow interconversion of these conformers could explain the reported coalescence in the ^{1}H and ^{13}C spectra.

Table 2
^{13}C chemical shifts of compounds **7**, **8**, **10**, **12**, **14–18** in methanol-d_4 and **18** also in dimethyl sulfoxide-d_6 (**18**[a]).

Atom no.	7	8	10	12	14	15	16	0	18	18[a]
1	37.4	30.0	34.3	39.5	36.1	42.1	37.7	38.1	39.2	37.8
2	68.7	29.1	68.5	72.8	70.8	70.3	68.7	70.0	109.0	107.8
3	68.5	65.6	70.3	73.7	72.5	73.5	68.0	68.6	72.3	70.1
4	32.9	33.3	36.2	27.6	24.7	27.5	35.9	33.2	35.1	34.0
5	51.9	52.4	80.4	133.6	49.0	133.7	49.7	54.1	53.1	51.2
6	206.3	206.2	202.3	144.2	202.7	144.6	199.1	215.0	204.8	202.4
7	122.6	122.4	120.1	181.2	125.3	180.9	144.8	39.8	122.6	120.8
8	166.6	167.1	166.1	124.7	158.8	133.0	118.7	123.8	153.8	152.4
9	35.2	35.3	39.1	165.5	76.2	168.2	137.1	137.4	83.2	80.7
10	39.3	37.7	45.5	42.2	43.7	42.6	41.9	44.3	48.9	47.3
11	21.7	22.1	22.7	25.6	29.1	25.4	125.9	23.8	31.5	29.7
12	31.1	31.4	31.2	36.7	28.4	28.4	40.9	37.0	28.7	26.9
13	48.9	49.4	49.0	48.1	49.0	49.2	48.0	47.5	49.65	47.8
14	85.1	85.3	84.9	140.3	86.4	82.1	142.2	147.3	87.3	84.9
15	32.2	32.1	32.1	127.4	31.7	33.7	134.1	120.1	31.2	29.9
16	22.3	22.4	22.2	33.6	22.1	23.8	33.9	32.7	22.2	20.6
17	60.2	60.3	60.1	63.9	60.1	58.5	64.5	66.0	59.7	57.9
18	17.6	17.6	17.6	18.3	17.6	18.1	20.0	17.8	18.4	17.3
19	24.5	24.5	17.1	27.6	19.8	28.6	30.9	29.6	21.0	20.3
20	212.6	212.5	212.5	211.9	212.4	213.4	211.4	211.6	212.5	209.3
21	31.6	31.6	31.6	31.6	31.6	31.7	31.4	31.5	31.5	31.1

The UV spectrum of compound **10** was practically identical with that of its parental compound, polypodine B (**4**), indicating no change in the chromophore. By means of MS, its molecular weight was established as m/z = 401 $[M + Na]^+$, suggesting that the side-chain was cleaved between C20-22, resulting in a molecular formula of $C_{21}H_{30}O_6$. The HPLC chromatogram along with the UV spectrum of compound **10** is available as Supplementary Information: Fig. S49, together with NMR spectra: Fig. S7–Fig. S14. In the hydrogen and carbon spectra, taken at 27 °C, no line-broadening were observed. The δH-9 = 3.23 ppm signal appeared as ddd multiplet with ^4J(H-9,H-7) = 2.5 Hz, ^3J(H-9,Hα-11) = 6.8 Hz and ^3J(H-9,Hβ-11) = 11.5 Hz couplings. In accordance with the expected structure of **10**, the DEPTQ spectrum (see Fig. S8) revealed the signals of three CH_3, six CH_2, four sp^3 CH, one =CH, and seven quaternary carbon atoms. Among the quaternary carbons, four sp^3 and three sp^2 hybrids could be identified. An inspection of the routine HSQC spectrum (Fig. S10 and S11) showed that the diastereotopic Hα-1 and Hβ-1 atoms are accidentally isochrones, whereas, due to the moderate resolution in the ^{13}C range, an adequate assignment of the C-11 and C-16 signals (22.7/22.2 ppm) is not possible. By utilizing the band-selective version of the two-dimensional HSQC measurement in the corresponding area (37–21 ppm) (Fig. S12), a perfect separation of the overlapping cross-peaks (δHα-11/δC-11: 1.89/22.7 and δHα-16/δC-16: 1.88/22.2) was accomplished. Differentiation between the α/β positions of hydrogen atoms of the methylene groups in the steroid core was achieved through one-dimensional selective ROESY experiments (Fig. S9). Irradiation of the δHα-9 = 3.23 ppm signal resulted ROE responses on Hα-2, Hα-4 and Hα-12, respectively, and this proved not only their signal assignment but also the retained *cis*-type junction of the A/B rings. Inserting the one-dimensional selROE on H-9 spectrum (see red line in Fig. S13) into the band-selective HSQC convincingly demonstrated the unambiguous differentiation of methylene groups in positions 11 and 17, despite their rather similar chemical shifts. The HMBC spectrum (Fig. S14) provided the H/C correlations ($^{2,3}J$(H,C). Considering the H_3-19/C and H_3-18/C section of HMBC (shown in Fig. S14), the cross-peaks of the H_3-19 methyl hydrogens unambiguously assigned signals of the quaternary C-5 and C-10, the tertiary C-9, and the secondary C-1, and the H_3-18 hydrogens assigned the quaternary C-13 and C-14, tertiary C-17 and secondary C-12 signals.

Compound **12** retained the characteristic UV spectrum of its parental compound calonysterone (**6**). The structural formula of compound **12** was established as $C_{21}H_{26}O_5$ by means of HRMS ($[M+H]^+$ calculated: 359.18530, found: 359.18602). HPLC chromatogram and UV spectrum of compound **12** are available as Supplementary Information: Fig. S51 together with NMR spectra: Fig. S15–Fig. S18. To facilitate the evaluation of the HSQC spectrum (Fig. S17) we have inserted the one-dimensional selTOCSY spectrum with irradiation on Hα-12 (see green line), from which the separately appearing Hα-11/Hβ-11 signals (2.73/2.65 ppm) assigned δC-11 at 25.6 ppm. To verify the δC-4 = 27.6 ppm assignment, we also utilized selROE on H_3-19 (see red line), where the ROE response at 2.54 ppm unambiguously marked out Hβ-4.

Compound **13** showed a slight hypsochromic shift in its UV spectrum as compared to that of poststerone (**7**), rising the suspicion that it might be a 9-hydroxylated derivative expectable to form analogously to our previous results on the autoxidation of 20E (**1**) [19]. The molecular formula was established as $C_{21}H_{30}O_6$ by means of HRMS ($[M+H]^+$ calculated: 379.21206, found: 379.21210). The ^1H and ^{13}C NMR spectra revealed this compound to be the analog of the natural product 9α,20-dihydroxyecdysone. The chemical shifts correlated well with the values of C-1 to C-16 reported earlier for this compound [28]. The δH_3-21 signal at 2.17 ppm, δC-21 and δC-20 peaks, at 31.6 and 212.3 ppm, respectively, demonstrate the presence of the CH_3-C=O group attached to C-17. HPLC chromatogram and UV spectrum of compound **13** is available as Supplementary Information (Fig. S52).

The UV spectrum of compound **14** was similar to that of **13**, and its molecular formula was also established as the same, $C_{21}H_{30}O_6$, by means of HRMS ($[M+H]^+$ calculated: 379.21206 found: 379.21246). HPLC chromatogram and UV spectrum of compound **14** are available as Supplementary Information: Fig. S53 together with NMR spectra: Fig. S19 − Fig. S23. In the DEPTQ measurement (Fig. S20) the C-9 signal remained under the noise level. The H_3-19/C-9 HMBC cross-peak (1.10/76.2 ppm, see Fig. S23) identified the C-9 signal whose high chemical shift of δC-9 = 76.2 ppm proved the OH substituent at this position. The selROE experiments (Fig. S21) on H_3-19 (see green line) and on H-5 (purple line) revealed the *trans* type A/B ring-junction and the Hα-5 configuration, evidencing that is this compound is the Hα-5 epimer of compound **13**.

Compound **15** exhibited a characteristic UV spectrum similar to that previously found for 14,15-dihydro-14α-hydroxycalonysterone, a product of the autoxidation of 20E (**1**) [19]. The molecular formula of compound **15** was established as $C_{21}H_{28}O_6$ by means of HRMS ($[M + H]^+$ calculated: 377.19641, found: 377.19621). HPLC chromatogram and UV spectrum of compound **15** are available as Supplementary Information: Fig. S54 together with NMR spectra: Fig. S24 − Fig. S28. The δH_3-21 signal at 2.17 ppm, δC-21 and δC-20 peaks, at 31.6 and 213.4 ppm, respectively, verified that the CH_3-C=O group attached to C-17 was retained. The appearance of a C=O signal at 180.9 ppm indicated its cross-conjugated arrangement. The HMBC (Fig. S28) correlations of H_3-19 (1.50/42.1 and 1.50/42.6, respectively) assigned the quaternary C-10 and H_2C-1 methylene moieties, furthermore the 1.50/133.7 and 1.50/168.2 responses proved the presence of quaternary sp^2 C= atoms in positions C-5 and C-9, which together showed the B ring as a $\Delta^{5,6}$-7-one-$\Delta^{8,9}$ chromophore. The δ^1H and $\delta^{13}C$ values of the A/B rings (see Table 1 and 2) of **15** correlate well with the corresponding values of **12**, revealing that both compounds contain the same structural moieties at this region. On the other hand, the HMBC cross-peak H_3-18/C-14 (0.66/82.1) of compound **15** revealed that, instead of the $\Delta^{14,15}$C = CH ethylene moiety (see structure **12** in Fig. 2), the HO-14α group of the parental poststerone **7** remained intact. Differentiation between the α/β positions of the diastereotopic methylene hydrogens of the skeleton was achieved by selective one-dimensional ROESY experiments (Fig. S26), irradiating the H_3-18 and H_3-19 atoms, respectively.

Compound **16** showed a characteristic UV spectrum similar to that previously found for isocalonysterone, the desmotropic pair of calonysterone (**6**), forming through the autoxidation of 20E (**1**) [19]. The molecular formula of compound **16** was established as $C_{21}H_{26}O_5$, the same as that of compound **12** ($[M+H]^+$ calculated: 359.18530, found: 359.18592). HPLC chromatogram and UV spectrum of compound **16** are available as Supplementary Information: Fig. S55 together with NMR spectra: Figs. S29 and S30. The ^1H and ^{13}C (APT) NMR spectra revealed this compound to be the 17-acetyl analog of isocalonysterone and the chemical shifts correlated well with the values of C-1 to C-16 reported earlier for isocalonysterone [19], moreover the signals of the 17 CH_3-C=O group were measured at δH_3-21 2.23 ppm, δC-21 and δC-20 peaks, at 31.4 and 211.4 ppm, respectively.

In case of compound **17**, the UV spectrum did not provide relevant structural information. The molecular formula of this compound was established as $C_{21}H_{28}O_4$ by means of HRMS ($[M + H]^+$ calculated: 345.20603, found: 345.20683). The number of double bond equivalents in compound **17** increased to eight, indicating that this compound contains one more double bound than its parent compound **7**. Twenty one ^{13}C signals were discernible in the DEPTQ spectrum of **17** (Fig. S32) indicating the presence of three methyl, six methylene, four sp^3 CH methyne and one sp^2 =CH groups, along with two quaternary sp^3 and five quaternary sp^2 carbon atoms, the latter including two non-conjugated C=O (δ 215.0 and 211.6 ppm) moieties. Integration of the signals in the ^1H NMR spectrum (Fig. S31) obtained in methanol-d_4 summed up to 26H atoms. Considering the nearly identical δC-2 and δC-3 chemical shifts of compound **17** and the parental **7**, both of these should have HO- substituents, and thus compound **17** contains 28 hydrogen atoms, coherently with the HRMS results. The HMBC (Fig. S35) correlations of H_3-19 (1.01/38.1, 1.01/44.3 and 1.01/54.1,

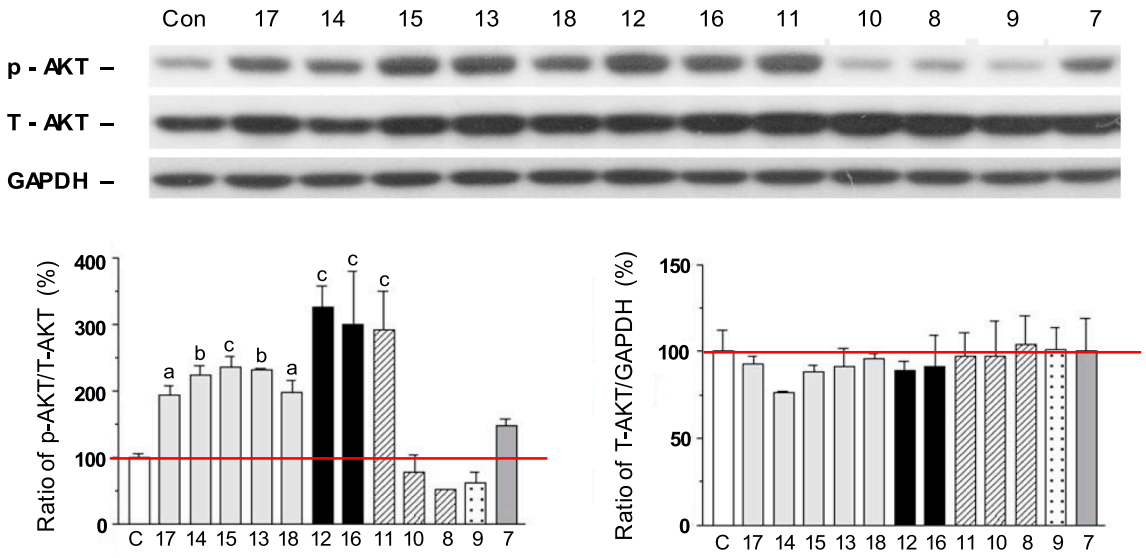

Fig. 3. Activity of compounds 7–18 as compared to the control (C) on the Akt phosphorylation in murine skeletal muscle myotubes. Quantification of Western blots was performed by ImageJ; error bars represent SEM from four parallel experiments. a: $p < 0.05$; b: $p < 0.01$; c: $p < 0.001$.

respectively) assigned the H_2C-1 methylene, the quaternary C-10 and HC-5 moieties, furthermore the 1.01/137.4 responses proved the presence of quaternary sp^2 =C atom in position C-9. The H_3-18 HMBC correlations assigned C-12, C-13 and C-16 atoms at 37.0, 47.5 and 65.0 ppm, respectively. Moreover, the 1.01/147.3 (H_3-18/C-14) correlation revealed the presence of a $\Delta^{14,15}$C = CH ethylene moiety in the D-ring of the steroid skeleton. The H-15/C-8 HMBC cross-peak established the $\Delta^{8,9}$ position of the second conjugated double bond. HMBC correlations of H-5 (2.49 dd, 12.8 and 4.0 Hz) verified the assignment of δO=C-6 (215.0 ppm) and δH_2C-7 (39.8 ppm) signals, respectively. Differentiation between the α/β hydrogens of the skeleton was achieved by selective one-dimensional ROESY experiments (Fig. S33), irradiating the H_3-18 and H_3-19 atoms. Checking the literary data revealed that compound **17** was formerly reported by Galbrait and his coworkers [29] in 1969 as a decomposition product of compound **7** after refluxing it in 0.5 N HCl in ethanol. Limited ^{1}H NMR data in $CDCl_3$ were given, and only the three methyl signals and the allyl hydrogen were assigned. Here we provide a complete ^{1}H and ^{13}C NMR signal assignment for this compound in methanol-d_4. HPLC chromatogram and UV spectra (Fig. S56), and the NMR spectra of compound **17** (Fig. S31–S35) are available as Supplementary Information.

Compound **18** also did not show analogous UV spectrum to any of the known autoxidized metabolites of 20E (**1**) [19]. HPLC chromatogram and UV spectrum of compound **18** are available as Supplementary Information (Fig. S57). According to our NMR protocol, first we performed the ^{1}H, DEPTQ, selROE, HSQC and HMBC measurements in methanol-d_4 (Supplementary Information: Figs. S36–S40). From these, we managed to assign the ^{13}C and ^{1}H signals of **18** in this solvent, certainly without the OH peaks. Taking into account the anomalous δC-2 = 109.0 ppm chemical shift of this quaternary carbon atom, attachment of a second oxygen substituent (e.g. –OH, –OOH, –OC) to C-2 was suspected. In analogous 9α-OH substituted ecdysteroids (e.g. **13** and **14**) the value of chemical shift for C-9 is expected around 76 ppm, but now in compound **18** it is δC-9 = 83.2 ppm, suggesting the presence of an -OOH or -OC substituent. To overcome this uncertainty, we evaporated the methanol solvent and all NMR investigations were subsequently performed in dimethyl sulfoxide-d_6 (Supplementary Information: Fig. S41–S45). In the DEPTQ spectrum (see Figs. S42), we identified the signals of three CH_3, six CH_2, three sp^3 CH, one =CH, and eight quaternary carbon atoms including five sp^3 and one sp^2 carbons, and two C=O groups. There are only three ^{1}H signals (6.63 s, 4.49 s and 5.00d (3.9 Hz) without ^1J(CH) correlation in the HSQC spectrum, proving the presence of three hydroxyl groups in compound **18**. The H_3-18/C and H_3-19/C HMBC correlations over two and three bonds ($^{2,3}J$(H,C)) provided the unequivocal assignment of C-12, C-13, C-14, and C-17 atoms, and C-1, C-5, C-9, and C-10 atoms, respectively (Fig. S45). The assignment of the detected hydroxyl signals to HO-2, HO-14 and HO-3 groups is straightforward on the basis of their HMBC cross-peaks. Whereas the HO- signal at 6.63 s shows ^3J(H,C) correlation with C-1 (37.8 ppm), this hydroxyl group is obviously connected to the quaternary C-2 (107.8 ppm). The second oxygen atom attached to this extremely deshielded C-2 forms a bridge to C-9 resulting a new five-membered ring in compound **18**. The second singlet HO-14 hydroxyl signal (4.49 s) showed cross-peaks not only with C-14, but also with the quaternary sp^2 C-8 (152.4 ppm), revealing the presence of the 6-one-$\Delta^{7,8}$ moiety. The H-7/C-5 and H-7/C-9 correlations completed the ^{13}C assignment. This way the molecular formula should be $C_{21}H_{28}O_6$ (DBE = 8), which was then subsequently supported by HRMS ([M + H]$^+$ calculated: 377.19586, found: 377.19625). One-dimensional selective ROESY experiments allowed differentiation between the α/β hydrogen atoms in the steroid core, and also proved the *cis*-type junction of the A/B rings (Fig. S43). To achieve an exact ^{1}H assignment even in case of strongly overlapping signals, the selTOCSY experiment was the method of choice. Irradiation on H-17 (3.20 ppm) resulted selectively the ^{1}H signals of the D-ring (see the green line inserted into the edHSQC spectrum of **18** in Fig. S44), whereas the experiment on Hα-12 (2.21 ppm) showed the spin system of the C-ring (inserted red line).

When comparing the oxidized products obtained from the base-catalyzed autoxidation of 20E (**1**) [19] with those obtained in this study from poststerone (**7**), the formation of both similar and different structures can be observed. Compound **12** was also one of the reaction products, even though with a lower yield than from the straightforward side-chain cleavage of calonysterone (**6**). Compounds **12–16** are the cleaved side-chain analogues of previously isolated compounds from the base-catalyzed autoxidation of 20E (**1**), while **17** and **18** represent the results of previously unobserved oxidative transformations.

2.3. Bioactivity on the Akt phosphorylation

The compounds were tested for their capacity to influence the Akt phosphorylation in murine C2C12 skeletal myotubes. The observed activities at 10 μM concentration are shown in Fig. 3.

With the exception of the side-chain cleaved derivatives of 2-deoxy-20-hydroxyecdysone (**2**), ajugasterone C (**3**) and polypodine B (**4**) (i.e. compounds **8**, **9** and **10**, respectively), all tested compounds demonstrated the ability to increase the activation of Akt. In particular, the side-chain cleaved analogs of dacryhainansterone (**5**), calonysterone (**6**) and isocalonysterone (i.e. compounds **11**, **12** and **16**, respectively) showed the strongest activity in this regard. All of these compounds express higher degree of unsaturation due to further conjugation extended to their D and/or C rings. This suggests that further double bonds conjugated with those present in the ecdysteroid B-ring may positively impact the bioactivities of these compounds in mammalian cells, and that such compounds might have stronger anabolic, anti-diabetic and anti-apoptotic activities than the more saturated ones including the abundant 20E (**1**) and its known *in vivo* metabolites [15]. On the other hand, when a separate experiment was performed to test poststerone (**7**) in comparison with 20E (**1**), it was found a weaker activator of Akt (293.3 ± 68.3% vs. 537.1 ± 25.3% activation at 10 μM, respectively, n = 6. Interestingly, however, poststerone (**7**) was also active at as low as 10 nM concentration (263.4 ± 69.6% activation, n = 6), where 20E (**1**) was already inactive. For the dose-dependency observed in this experiment, see Supplementary Information, Fig. S58.

The well-known role of Akt in driving cancer [30] should also be taken into account when interpreting such bioactivity results. At this point it is impossible to make a sound judgment whether or not a stronger *in vitro* activation of this protein kinase would have *in vivo* relevance, and particularly if this would confer ecdysteroid metabolites any pro-cancerous risk. Current experiences with the apparent safety of ingesting large (up to several grams) doses of ecdysteroids by sportsmen at least do not seem to raise concerns, even though long-term safety of such a practice has never been studied in humans. Nevertheless, our results clearly show that side-chain cleaved metabolites of ecdysteroids accompanying 20E (**1**) within plant extracts have all the potential to significantly contribute to the complex bioactivity.

3. Conclusions

By using two different chemical strategies (oxidative side-chain cleavage of various phytoecdysteroids and autoxidation of poststerone), a set of semi-synthetic side-chain cleaved ecdysteroids was obtained from acceptable to good yields. In particular, poststerone could be obtained with an isolated yield of as high as 81.35%. Comprehensive NMR spectroscopic techniques allowed a complete signal assignment for each new compound. Several of the new compounds are derivatives of known phytoecdysteroids with an intact side-chain. Since the side-chain cleavage is a known metabolic step of 20E in rodents, the prepared compounds can be assumed as potential *in vivo* metabolites of the corresponding phytoecdysteroids.

The compounds showed the ability to increase the activation of protein kinase B in C2C12 myotubes in murine skeletal muscle cells. Our results suggest that, similarly to our most recent results with poststerone, the metabolic step of side-chain cleavage leads to compounds with altered, and apparently increased bioactivity in mammals. Such compounds can reasonably be expected to significantly contribute to the overall activity observed after the consumption of preparations (e.g. food supplements) containing a variety of phytoecdysteroids. Moreover, these metabolites are potentially valuable leads towards possible ecdysteroid-inspired drug discovery initiatives.

4. Materials and methods

4.1. Starting materials

20-Hydroxyecdysone (**1**) with a purity of 90%, originated from the roots of *Cyanotis arachnoidea* was purchased from Shaanxi KingSci Biotechnology Co., Ltd. (Shanghai, China). A purification step was performed by recrystallization from ethyl acetate - methanol (2:1, v/v) to reach a 97.8% purity by means of RP-HPLC.

2-Deoxy-20-hydroxyecdysone (**2**) was previously isolated by our research group from *Silene italica ssp. nemoralis* [31], ajugasterone C (**3**), polypodine B (**4**) were obtained from our previous isolation from *Serratula wolffii* [32]. Compounds **2**, **3** and **4** possessed a purity of > 95% by means of RP-HPLC. Dacryhainansterone (**5**) and calonysterone (**6**) were isolated in our laboratory with a purity of 99.1% and 99.7%, respectively, from a commercial extract of *Cyanotis arachnoidea* [33].

4.2. General methods

All reagents and solvents were obtained from commercially available sources and were used without further purification.

Reactions' progress were monitored by NP-TLC performed on silica plates (Silica gel 60F254, E. Merck, Germany), by using the solvent system composed of ethyl acetate - ethanol - water (12:1:0.5, v/v/v). Visualizations were performed under UV light λ_1 = 254 nm and after spraying with vanillin/sulfuric acid reagent under λ_2 = 365 nm.

Compounds were fractionated and/or purified by using different chromatographic techniques. RP-HPLC for semi-preparative purifications was carried out on an Agilent 1100 series (Waters Co., Milford, MA, USA) connected to a Jasco UV-2075 detector (Jasco Co., Tokyo, Japan). RP-HPLC for preparative purifications was performed on a Waters 600 Pump connected to a Waters 2487 Dual λ Absorbance Detector (Waters Co., Milford, MA, USA). Rotation planar chromatography was performed on a Chromatotron device (Harrison Research, Palo Alto, CA, USA). Flash chromatography was performed on a CombiFlash® Rf + apparatus (Teledyne Isco, Lincoln, USA) with an 80 g HP Silica RediSep® Rf Gold column (Teledyne Isco, Lincoln, USA). Centrifugal Partition Chromatography was performed on an Armen Spot CPC 250 ml (Armen Instrument, Saint Ave, France) system composed of an Armen Spot Prep II equipment and an Armen Spot CPC multilayer coil separation column, and controlled by the Armen Glider CPC software. Optimization of the CPC separation was through following well-established general concepts published in the literature [33–36].

Purity of the obtained compounds was determined by RP-HPLC analyses on a system of two Jasco PU-2080 pumps, a Jasco AS-2055Plus intelligent sampler connected to a JASCO LC-Net II/ADC equipped with a Jasco MD-2010 Plus PDA detector (Jasco Co., Tokyo, Japan). Turbo ion spray tandem MS of compounds **8** and **10** were recorded on a API 2000 triple quadrupole tandem mass spectrometer (AB SCIEX, Foster City, CA, USA) equipped with ESI ion source that was used in the positive mode. HRMS data for compounds **12–18** were recorded on a Waters Acquity I-Class UHPLC system (Waters Co., Milford, MA, USA) coupled with a Thermo Scientific Q Exactive Plus Orbitrap mass spectrometer equipped with HESI ion source (Thermo Fisher Scientific, Scoresby, Australia).

^{1}H (500.1 MHz) and ^{13}C (125.6 MHz) NMR spectra of compounds were recorded at room temperature on a Bruker 500 Avance III NMR spectrometer equipped with cryogenic probe head, or on a Bruker Avance 500 NMR spectrometer. Amounts of approximately 0.7–5 mg of compounds were dissolved in 0.1 ml of methanol-d_4 and transferred to 2.5 mm Bruker MATCH NMR sample tube (Bruker). Chemical shifts are given on the δ-scale and are referenced to the solvent (methanol-d_4: δ_C = 49.1 and δ_H = 3.31 ppm). NMR data of compound **18** were also determined in dimethyl sulfoxide-d_6 (δ_C = 39.5 and δ_H = 2.50 ppm). Pulse programs of all experiments (one-dimensional ^{1}H, ^{13}C, DEPTQ, DEPT-135, APT, sel-TOCSY, sel-ROE (τ_{mix}: 300 ms), two-dimensional ^{1}H,^{1}H-COSY, gs-HSQC, edited gs-HSQC, gs-HMBC and band-selective HSQC and band-selective HMBC) were taken from the Bruker software library.

4.3. Synthesis

4.3.1. Synthesis of compounds 7–12 through oxidative side-chain cleavage of phytoecdysteroids 1–6

Synthesis of poststerone (7). 20-hydroxyecdysone (**1**) was used as starting material for the synthesis of poststerone (**7**). 5.0 g of 20E (**1**) was dissolved in 400 ml of methanol, 1 equiv. of PIDA was added, and the solution was stirred at room temperature for 45 min. The reaction mixture was then neutralized with a 5% aqueous solution of $NaHCO_3$, and the solvent was evaporated at 40 °C under vacuum. The residue was dissolved in methanol, and 12 g of silica powder was added. The solvent was evaporated under vacuum, and the dried extract adsorbed onto silica ('dried solid sample loading' technique) was transferred to a universal Rf cartridge (Teledyne Isco, Lincoln, USA). For the purification, flash chromatography was used with a mobile phase of *n*-hexane - dichloromethane (6:4, v/v; solvent A), and dichloromethane - methanol (1:1, v/v; solvent B), and a 40 min gradient program of 0–30% B in A was applied at a flow rate of 60 ml/min. Compound **7** was obtained with an isolated yield of 81.41% (3.07 g).

General procedure for the synthesis of compounds 8–11. Compounds **2–5** were used as starting materials for the synthesis of compounds **8**, **9**, **10** and **11**, respectively. Each starting material (**2–5**) was dissolved in methanol to a final concentration of 100 mM (**2**, **5**: 46 mg; **3**: 48 mg; **4**: 50 mg), and 1.2 equiv. of PIFA was added. The mixtures were stirred for 60 min at room temperature. The reactions were stopped by neutralizing the pH by using a 5% aqueous solution of $NaHCO_3$, followed by evaporation to dryness. Each residue was dissolved in ethyl acetate and filtered through silica, then dried. Compounds **8** and **9** were purified over preparative RP-HPLC applying a Kinetex XB-C18 (5 µm, 250 x 21.2 mm) column with 50% aqueous methanol as eluent at a flow rate of 10 ml/min, detecting at 254 nm. Compounds **8** and **9** were isolated at 56.4% (19.5 mg) and 62.6% (22.7 mg) yields, respectively. Compounds **10** and **11** were purified over RPC using a four-step gradient elution with cyclohexane - ethyl acetate (1:1 and 1:5, v/v) and ethyl acetate - ethanol (12:1 and 6:1, v/v), with 80 ml for each solvent, and 23 fractions were collected. Compounds **10** and **11** were obtained at 60.2% (21.6 mg) and 59.5% (22.7 mg) yield, respectively.

Synthesis of compound 12. Calonysterone (**6**) was used as starting material for the synthesis of compound **12**. 50 mg of calonysterone (**6**) was dissolved in 12.5 ml methanol, 1 equiv. of PIDA was added, and the solution was stirred at room temperature for 60 min. The reaction was stopped by adjusting the pH of the final mixture to neutral with a 5% aqueous solution of $NaHCO_3$. After evaporation of the solvent under nitrogen, the residue was purified by CPC in ascending mode with a biphasic solvent system composed of *n*-hexane - ethyl acetate - methanol - water (3:10:3:10, v/v/v/v). The solvent system offered the following separation characteristics: a very short settling time (17 s), the volume ratio of the upper and lower phases was 0.86, and the retention volume ratio Sf was 0.68. The equipment optimized parameters were as follows: constant pressure of 86 bars, flow rate of 10 ml/min, and rotation speed of 2600 rpm. The purification was performed through a single injection and an altogether 94.42% of the initial weight was recovered after the separation. Compound **12** was obtained with a yield of 51.8% (19.5 mg).

4.3.2. Synthesis of compounds 12–18 through base-catalyzed autoxidation of poststerone (7)

The base-catalyzed autoxidation of poststerone (**7**) was performed by dissolving 450 mg of poststerone (**7**) in a mixture of 10 ml of MeOH and 80 ml of water, then 500 mg of NaOH dissolved in 10 ml of water was added. The reaction mixture was stirred for 4 h at room temperature, and the reaction was stopped by neutralizing the mixture with a 9.6% aqueous solution of acetic acid. After evaporating the solvent under nitrogen stream, the residue was pre-purified by solid-phase extraction through silica using methanol as eluent, then dried.

The reaction mixture was subsequently fractionated by CPC in ascending mode, by using the biphasic solvent system previously developed in our laboratory for the separation of 20E (**1**) and its oxidized derivatives [19]; it was composed of ethyl acetate - water - methanol (20:20:1, v/v/v). The equipment optimized parameters were settled as follows: constant pressure of 80 bar, flow rate of 10 ml/min and rotation speed of 2900 rpm. The fractionation was performed through four consecutive injections, and an altogether 95.43% of the initial weight was recovered after the separation. The CPC fractions were combined based on their NP-TLC fingerprints, evaporated under vacuum at 40 °C, dissolved in methanol and investigated by RP-HPLC on a Kinetex XB C-18 (5 µm, 250 × 4.6 mm) column with an isocratic solvent system of 23% aqueous acetonitrile at a flow rate of 1 ml/min. Fractions 6, 7 and combined fractions 11–13 were selected for additional purification steps. Fraction 6 was further purified over semi-preparative RP-HPLC with 30% aqueous acetonitrile at a flow rate of 3 ml/min using a Gemini C18 (5 µm, 250 × 10 mm) column to yield compounds **12** (1.5 mg, 0.34%) and **16** (3.76 mg, 0.84%). Fraction 7 was further purified over semi-preparative RP-HPLC with 27% aqueous acetonitrile at a flow rate of 3 ml/min using a Gemini C18 (5 µm, 250 × 10 mm) column to yield compound **17** (10.61 mg, 2.48%). The CPC combined fractions 11–13 were further purified over semi-preparative RP-HPLC with 20% aqueous acetonitrile at a flow rate of 3 ml/min using a Luna Phenyl-Hexyl (5 µm, 250 × 10 mm) column to yield compounds **13** (10.2 mg, 2.17%), **14** (5.7 mg, 1.21%), **15** (11.3 mg, 2.42%) and **18** (4.6 mg, 1.00%).

In order to obtain more amounts of the above compounds, the reaction was repeated by using another 500 mg of poststerone (**7**) that was stirred for 7 h, and the work-up procedure consisted of the same purification steps as detailed above. The isolated yields in this case were as follows: compound **13** (27.9 mg, 5.34%), compound **14** (3.04 mg, 0.58%), compound **15** (20 mg, 3.85%), compound **16** (20 mg, 4.04%) and compound **18** (5.72 mg, 1.1%).

4.4. Bioactivity testing

Mouse C2C12 skeletal myoblasts (BCRC#60083) were purchased from the Bioresource Collection and Research Center (BCRC, Food Industry Research and Development Institute, Taiwan). The cells were seeded in 6-well plates and maintained in high-glucose Dulbecco's modified Eagle's medium (DMEM) with 10% fetal bovine serum and 1% penicillin/streptomycin solution in a humidified atmosphere of 95% air and 5% CO_2 at 37 °C. After reaching 100% confluence, C2C12 myoblasts were cultured in differentiation medium (DMEM containing 4500 mg/L D-glucose and 10% horse serum), and the medium was changed every 2 days. The cells became skeletal myotubes after 8 days of differentiation. Then, the culture medium was changed to serum free normal-glucose DMEM with or without 10 µM of each test compound. After 2 h, the cells were lysed with 500 µL of 1 × sample buffer (62.5 mM Tris-HCl, pH 6.8; 10% glycerol; 2% SDS; 50 mM DTT; 0.0025% bromophenol blue), sonicated for 10–15 s, and heated to 95–100 °C for 5 min. For analysis of AKT activation, the cell lysate was loaded and separated on 10% SDS-polyacrylamide gels. Proteins were then transferred to PVDF membranes and detected using phosphorylated and total Akt antibodies (Cell Signaling Technology, Inc., Danvers, MA, USA).

Acknowledgements

A.H. acknowledges the János Bolyai fellowship of the Hungarian Academy of Sciences and the Kálmán Szász Prize. The authors wish to thank Mr. Attila Csorba (Institute of Pharmacognosy, University of Szeged) for the HRMS measurements.

Funding

This work was supported by the National Research, Development

and Innovation Office, Hungary (NKFIH; K119770), and by the Ministry of Science and Technology, Taiwan (MOST 104-2314-B-037-067). The authors acknowledge support from the Ministry of Human Capacities, Hungary grant 20391-3/2018/FEKUSTRAT, the EU-funded Hungarian grant EFOP-3.6.1-16-2016-00008, and GINOP-2.3.2-15-2016-00012, and from a bilateral mobility grant from the Hungarian Academy of Sciences and the Ministry of Science and Technology, Taiwan (MOST 107-2911-I-037-502).

Appendix A. Supplementary material

Supplementary data to this article can be found online at https://doi.org/10.1016/j.bioorg.2018.10.049.

References

[1] R. Lafont, J. Harmatha, F. Marion-Poll, L. Dinan, I.D. Wilson, Ecdybase: a free ecdysteroid database. http://ecdybase.org/, 2002 → continuously updated (accessed 05 July 2018).
[2] L. Dinan, Phytoecdysteroids: biological aspects, Phytochemistry 57 (2001) 325–339, https://doi.org/10.1016/S0031-9422(01)00078-4.
[3] M.J. Klowden, Academic Press, Signaling systems in Physiological Systems in Insects, Physiological Systems in Insects, Elsevier Science & Technology, London, 2013, pp. 1–87.
[4] L. Dinan, The Karlson lecture. phytoecdysteroids: what use are they, Arch. Insect Biochem. Physiol. 72 (2009) 126–141, https://doi.org/10.1002/arch.20334.
[5] G. Laekeman, A. Vlietinck, Phytoecdysteroids: Phytochemistry and Pharmacological Activity, in: K.G. Ramawat, J.M. Merillon (Eds.), Natural products: phytochemistry, botany and metabolism of alkaloids, phenolics and terpenes, Springer, Berlin, 2013, pp. 3827–3850.
[6] M. Báthori, N. Tóth, A. Hunyadi, A. Márki, E. Zádor, Phytoecdysteroids and anabolic-androgenic steroids-structure and effects on humans, Curr. Med. Chem. 15 (2008) 75–91, https://doi.org/10.2174/092986708783330674.
[7] Q. Chen, Y. Xia, Z. Qiu, Effect of ecdysterone on glucose metabolism in vitro, Life Sci. 78 (2006) 1108–1113, https://doi.org/10.1016/j.lfs.2005.06.031.
[8] P. Kizelsztein, D. Govorko, S. Komarnytsky, A. Evans, Z. Wang, W.T. Cefalu, I. Raskin, 20-Hydroxyecdysone decreases weight and hyperglycemia in a diet-induced obesity mice model, Am. J. Physiol. Endocrinol. Metab. 296 (2009) E433–E439, https://doi.org/10.1152/ajpendo.90772.2008.
[9] T.A. Kutepova, V.N. Syrov, Z.A. Khushbaktova, Z. Saatov, Hypoglycemic activity of the total ecdysteroid extract from *Ajuga turkestanica*, Pharm. Chem. J. 35 (2001) 608–609, https://doi.org/10.1023/A:1015145811009.
[10] K. Hamden, F. Ayadi, K. Jamoussi, H. Masmoudi, A. Elfeki, Therapeutic effect of phytoecdysteroids rich extract from *Ajuga iva* on alloxan induced diabetic rats liver, kidney and pancreas, BioFactors 33 (2008) 165–175, https://doi.org/10.1002/biof.5520330302.
[11] I. Todorov, Y. Mitrokin, O. Efremova, L. Sidorenko, The effect of ecdysterone on the biosynthesis of proteins and nucleic acids in mice, Pharm. Chem. J. 34 (2000) 455–458, https://doi.org/10.1021/jf073059z.
[12] J. Gorelick-Feldman, D. MacLean, N. Ilic, A. Poulev, M.A. Lila, D. Cheng, I. Raskin, Phytoecdysteroids increase protein synthesis in skeletal muscle cells, J. Agric. Food. Chem. 56 (2008) 3532–3537, https://doi.org/10.1021/jf073059z.
[13] N. Tóth, A. Szabó, P. Kacsala, J. Héger, E. Zádor, 20-Hydroxyecdysone increases fiber size in a muscle-specific fashion in rat, Phytomedicine 15 (2008) 691–698, https://doi.org/10.1016/j.phymed.2008.04.015.
[14] J. Gorelick-Feldman, W. Cohick, I. Raskin, Ecdysteroids elicit a rapid Ca^{2+} flux leading to Akt activation and increased protein synthesis in skeletal muscle cells, Steroids 75 (2010) 632–637, https://doi.org/10.1016/j.steroids.2010.03.008.
[15] S. Schiaffino, C. Mammucari, Regulation of skeletal muscle growth by the IGF1-Akt/PKB pathway: insights from genetic models Skeletal, Muscle 1 (4) (2011), https://doi.org/10.1186/2044-5040-1-4.
[16] M. Sandri, L. Barberi, A.Y. Bijlsma, B. Blaauw, K.A. Dyar, G. Milan, C. Mammucari, C.G.M. Meskers, G. Pallafacchina, A. Paoli, D. Pion, M. Roceri, V. Romanello, A.L. Serrano, L. Toniolo, L. Larsson, A.B. Maier, P. Muñoz-Cánoves, A. Musarò, M. Pende, C. Reggiani, R. Rizzuto, S. Schiaffino, Signalling pathways regulating muscle mass in ageing skeletal muscle. The role of the IGF1-Akt-mTOR-FoxO pathway, Biogerontology 14 (2013) 303–323, https://doi.org/10.1007/s10522-013-9432-9.
[17] S. Kumpun, J.P. Girault, L. Dinan, C. Blais, A. Maria, C. Dauphin-Villemant, B. Yingyongnarongkul, A. Suksamrarn, R. Lafont, The metabolism of 20-hydroxyecdysone in mice: relevance to pharmacological effects and gene switch applications of ecdysteroids, J. Steroid Biochem. Mol. Biol. 126 (2011) 1–9, https://doi.org/10.1016/j.jsbmb.2011.03.016.
[18] A. Suksamrarn, P. Ganpinyo, C. Sommechai, Base-catalyzed autoxidation of 20-hydroxyecdysone: synthesis of calonysterone and 9,20-dihydroxyecdysone, Tetrahedron Lett. 35 (1994) 4445–4448, https://doi.org/10.1016/S0040-4039(00)73380-6.
[19] J. Csábi, T.J. Hsieh, F. Hasanpour, A. Martins, Z. Kele, T. Gáti, A. Simon, G. Tóth, A. Hunyadi, Oxidized metabolites of 20-hydroxyecdysone and their activity on skeletal muscle cells: preparation of a pair of desmotropes with opposite bioactivities, J. Nat. Prod. 78 (2015) 2339–2345, https://doi.org/10.1021/acs.jnatprod.5b00249.
[20] J.B. Siddall, D.H.S. Horn, E.J. Middleton, Synthetic studies on insect hormones. The synthesis of a possible metabolite of crustecdysone (20-hydroxyecdysone), Chem. Commun. (1967) 899–900, https://doi.org/10.1039/C19670000899.
[21] R.Q. Petersen, R.C. Cambie, G.B. Russell, Jones oxidation of 20-hydroxyecdysone (crustecdysone), Aust. J. Chem. 46 (1993) 1961–1964, https://doi.org/10.1071/CH9931961.
[22] A. Hunyadi, J. Csábi, A. Martins, J. Molnár, A. Balázs, G. Tóth, Backstabbing P-gp: side-chain cleaved ecdysteroid 2,3-dioxolanes hyper-sensitize MDR cancer cells to doxorubicin without efflux inhibition, Molecules 22 (2017) 199, https://doi.org/10.3390/molecules22020199.
[23] H. Duddeck, W. Dietrich, G. Tóth, Structure Elucidation by Modern NMR, Springer-Steinkopff-Verlag, Heidelberg, 1998.
[24] E. Pretsch, G. Tóth, M.E. Munk, M. Badertscher, Computer-Aided Structure Elucidation, Spectra Interpretation and Structure Generation, Wiley-VCH, Weinheim, 2002.
[25] A. Hunyadi, G. Tóth, A. Simon, M. Mák, Z. Kele, I. Máthé, M. Báthori, Two new ecdysteroids from Serratula wolffii, J. Nat. Prod. 67 (2004) 1070–1072, https://doi.org/10.1021/np030544p.
[26] A. Martins, N. Tóth, A. Ványolós, Z. Béni, I. Zupkó, J. Molnár, M. Báthori, A. Hunyadi, Significant activity of ecdysteroids on the resistance to doxorubicin in mammalian cancer cells expressing the human ABCB1 transporter, J. Med. Chem. 55 (2012) 5034–5043, https://doi.org/10.1021/jm300424n.
[27] M. Vágvölgyi, A. Martins, Á. Kulmány, I. Zupkó, T. Gáti, A. Simon, G. Tóth, A. Hunyadi, Nitrogen-containing ecdysteroid derivatives vs. multi-drug resistance in cancer: preparation and antitumor activity of oximes, oxime ethers and a lactam, Eur. J. Med. Chem. 144 (2018) 730–739, https://doi.org/10.1016/j.ejmech.2017.12.032.
[28] Z. Pongrácz, M. Báthori, G. Tóth, A. Simon, M. Mák, I. Máthé, 9α,20-Dihydroxyecdysone, a new natural ecdysteroid from Silene italica ssp. nemoralis, J. Nat. Prod. 66 (2003) 450–451, https://doi.org/10.1021/np0205194.
[29] M.N. Galbraith, D.H.S. Horn, E.J. Middleton, The structure of podecdysone B, a new phytoecdysone, J. Chem. Soc. (1969) 402–403, https://doi.org/10.1039/C29690000402.
[30] P.S. Mundi, J. Sachdev, C. McCourt, K. Kalinsky, AKT in cancer: new molecular insights and advances in drug development, Br. J. Clin. Pharmacol. 82 (2016) 943–956, https://doi.org/10.1111/bcp.13021.
[31] N. Tóth, A. Simon, G. Tóth, Z. Kele, A. Hunyadi, M. Báthori, 26-Hydroxylated ecdysteroids from *Silene viridiflora*, J. Nat. Prod. 71 (2008) 1461–1463, https://doi.org/10.1021/np800139q.
[32] A. Hunyadi, A. Gergely, A. Simon, G. Tóth, G. Veress, M. Báthori, Preparative-scale chromatography of ecdysteroids of *Serratula wolffii* Andrae, J. Chromatogr. Sci. 45 (2007) 76–86, https://doi.org/10.1093/chromsci/45.2.76.
[33] H.M. Issaadi, Y.C. Tsai, F.R. Chang, A. Hunyadi, Centrifugal partition chromatography in the isolation of minor ecdysteroids from *Cyanotis arachnoidea*, J. Chromatog. B 1054 (2017) 44–49, https://doi.org/10.1016/j.jchromb.2017.03.043.
[34] J.B. Friesen, J.B. McAlpine, S.N. Chen, G.F. Paulin, Countercurrent separation of natural products: an update, J. Nat. Prod. 78 (2015) 1765–1796, https://doi.org/10.1021/np501065h.
[35] J. Cazes, Encyclopedia of Chromatography 2004 Update Supplement, Marcel Dekker Inc, New York, 2003.
[36] M. Bojczuk, D. Żyżelewicz, P. Hodurek, Centrifugal partition chromatography - a review of recent applications and some classic references, J. Sep. Sci. 40 (2017) 1597–1609, https://doi.org/10.1002/jssc.201601221.